

Numerical analysis of the mean flow effect on the sound directivity pattern of cylindrical ducts

Yong Shi

Centre for Interdisciplinary Research
in Music Media and Technology,
McGill University,
Canada
yong.shi2@mail.mcgill.ca

Andrey da Silva

Centro de Engenharia da Mobilidade,
Federal University of Santa Catarina,
Brazil
andrey.rs@ufsc.br

Gary Scavone

Centre for Interdisciplinary Research
in Music Media and Technology,
McGill University,
Canada
gary@music.mcgill.ca

ABSTRACT

This paper presents a numerical investigation of the sound directivity pattern of normal modes radiated from the open end of a cylindrical pipe. A good agreement is found between the numerical results and the analytical predictions of the directivity pattern for an unflanged pipe in the absence and in the presence of a low Mach-number mean flow. The investigations are conducted by using an axisymmetric two-dimensional lattice Boltzmann model. The numerical model is first validated by comparing its directivity with the established analytical model by Levine and Schwinger [1] for the case of zero mean flow. Then the numerical results under the condition of mean flow with two different Mach numbers are compared with the analytical model by Gabard and Astley [2] and recent experimental observations by Gorazd et al [3]. The effects of the so-called zone of relative silence are observed in the results even for very low Mach number ($M = 0.036$).

1. INTRODUCTION

The directivity characteristics of the acoustic wave radiating from the open end of cylindrical ducts have been investigated by many researchers over the last century. Much attention has been focused on engineering cases, such as exhaust pipes, ventilation systems, air-conditioning systems, etc. For musical instrument makers and researchers of woodwind musical instruments, the direction-dependent sound radiation characteristics of the external sound field are also of great interest. This problem can be investigated by analytical, experimental, and numerical approaches.

Levine and Schwinger [1] proposed an analytical model for the dominant mode propagation of sound out of a semi-infinite circular duct in the absence of flow. Their solution is based on the Wiener-Hopf technique, and gives rigorous and explicit results including the reflection coefficient R , the length correction l/a and the angular distribution of the emitted sound radiation described as the power gain function $G(\theta)$.

In the so-called outlet problems, the sound propagation out of a pipe carrying a non-zero mean flow is more complex due to the interaction between the sound field and the fluid field. Assuming a uniform flow, a thin vortex sheet separating the jet and the surrounding fluid and a full Kutta condition¹ at the edges of the open end, Munt [4] proposed an expression for the far-field sound radiation for the range of $0 \leq ka \leq 1.5$ and $M < 0.3$, which also uses the Wiener-Hopf technique and can be seen as an extension of Levine and Schwinger's model. This solution was elaborated by Rienstra [5] who introduced a complex parameter to take into account the effects of unsteady shedding of vorticity in the vicinity of the trailing edge, with particular attention to the energy balance of the sound field and the fluid field. Savkar [6] also presented an approximate model for the sound radiation from a semi-infinite circular duct by using a Wiener-Hopf analysis solved by an approximate method. Based on the work of both Munt and Rienstra, Gabard and Astley [2] presented an extended model that includes a center body for the cases of annular pipe and proposed an explicit numerical procedure for evaluating the solutions for higher frequencies (ka in the range of $0 - 60$ and higher Mach numbers (in the range of $0 - 0.8$). The pressure directivity of any single mode or all modes combined together can be derived from each of the analytical models cited above.

The analytical models are useful for problems involving simple geometries and as benchmark solutions for numerical simulations and experimental measurements. In realistic situations, however, the geometric characteristics of outlet systems, such as tailpipes and woodwind instruments, are not limited to simple geometries such as the unflanged circular duct. For cases of complex geometries, numerical approaches are more suitable.

In a recent example, Hornikx et al. [7] presented a numerical solution for calculating the radiation sound field emanating from an automotive exhaust pipe above a rigid surface. Other examples of numerical methods for problems of sound radiation can be found in [8], [9] and [10], to name just a few.

For the particular problems to be investigated in this paper, a numerical approach in the time domain called the lattice Boltzmann method (LBM) is used. The LBM is very different from the traditional continuum-based techniques

Copyright: ©2013 Yong Shi et al. This is an open-access article distributed under the terms of the [Creative Commons Attribution 3.0 Unported License](https://creativecommons.org/licenses/by/3.0/), which permits unrestricted use, distribution, and reproduction in any medium, provided the original author and source are credited.

¹ The vortex layer leaves the edge of the cylinder with zero gradient.

in that it directly simulates the propagation and collision involving the space-time evolution of the fluid particles in a mesoscopic level rather than the pressure and velocity in a macroscopic level. Here the particles are not real atoms or molecules but rather velocity distribution functions representing the probability of finding a population of fluid molecules in a certain phase space.

The dynamic behavior of the populations are governed by a space-temporal discretization of the Boltzmann equation, known as the lattice Boltzmann equation (LBE). The macroscopic fluid properties, such as density, momentum, internal energy, and energy flux, can be recovered from the moments of the velocity distribution functions. Since the Boltzmann equation describes the physical phenomena of a fluid at a lower level and a smaller time scale, the Navier-Stokes equations can be fully recovered from the Boltzmann equation. The numerical solution of the Boltzmann equation is relatively simple compared to the Navier-Stokes equations, and can be implemented in a parallel computation scheme. This is advantageous for simulations of problems featuring complicated boundary conditions and multiphase interfaces.

The LBM has been extensively used in hydrodynamic problems, but only a few researchers have used the LBM in the field of wind musical instruments and musical acoustics. Skordos [11] first simulated the interaction between fluid flow and the acoustic waves within a flute-like instrument at different blowing speeds by using a two-dimensional lattice Boltzmann model.

In a series of simulations, da Silva et al [12–15] investigated the sound radiation at the open end of axisymmetric cylindrical pipes in terms of reflection coefficient, length correction and directivity factor. In [12], the sound radiation of the unflanged cylinder pipe immersed in a stagnant fluid is simulated. The simulation results in terms of $|R|$, l/a and radiation directivity agree well with the analytical model for inviscid wave propagation by Levine and Schwinger [1]. In [14], they investigated the influence of a cold subsonic mean flow of low Mach number in the stagnant fluid, as well as the effects of circular horns of different radii of curvature at the open end of the cylindrical pipe. Their simulation correctly demonstrates that a free laminar jet is formed downstream from the open end due to discharge of the upstream mean flow into the radiation area. For the case of an unflanged pipe, the simulation data in terms of $|R|$ and l/a agrees well with the analytical solution proposed by Munt [16] and the experimental data obtained by Allam and Abom [17], where the maximum value of the reflection coefficient is greater than one due to the energy exchange between the vortex sheet and the acoustic field. For the case of circular horns, their simulation data is in accordance with the experiments carried out by Peters et al. [18]. In a similar simulation [15], they investigated a more realistic case of the effects of mean flow corresponding to different dynamic playing levels for a cylindrical pipe terminated by a catenoidal horn. The series investigations conducted by da Silva et al. demonstrate that the lattice Boltzmann technique is a reliable numerical tool for investigating musical acoustics problems that in-

volve a radiating waveguide and a low Mach number fluid flow.

The objective of this paper is to investigate the pressure directivity of sound waves as they propagate into the far field from the open end of a cylindrical duct issuing a subsonic cold mean flow. The investigations are conducted by using the lattice Boltzmann method to represent a two-dimensional radiation domain. This paper is structured as follows: Section 2 describes the numerical technique used in the study. In Section 3, the simulation results are compared to the analytical model by Levine and Schwinger and the experimental observations by Gorazd et al. for the case of no flow, and to the analytical model by Gabard and Astley and the experimental observations by Gorazd et al. for the case of low Mach number mean flow. The phenomenon of the zone of relative silence is discussed for two different Mach numbers. Finally, Section 4 provides a discussion of the results and suggestions for further investigations.

2. NUMERICAL PROCEDURE

The purpose of the LBM scheme presented here is to reproduce the sound radiation at the open end of a cylindrical duct in the presence of a low Mach subsonic cold mean flow. General descriptions of the lattice Boltzmann method can be found in books by Succi [19] and Gladrow [20].

The LBM scheme is described by an axisymmetric cylinder structure immersed in a fluid domain surrounded by open boundaries, as illustrated in Fig. 1. The fluid domain defined by an axisymmetric half-plane is represented by a rectangular D2Q9 structure [21] of 1000 by 500 lattice cells. The left, top and right boundaries of the radiation domain are implemented by absorbing boundary conditions prescribed with a zero velocity, as proposed by Kam et al. [22]. The boundary representing the axis of symmetry of the system, along the bottom, is implemented by a free-slip boundary condition. The axisymmetric nature of the system is recovered by using an axisymmetric source term [23, 24].

The length and the radius of the cylindrical waveguide is $L = 469.5$ and $a = 10$ in lattice cells, respectively. The walls of the waveguide are represented by a boundary of zero thickness [25, 26]. The outer walls are treated by a simple bounce-back scheme [19] for which the viscous boundary phenomena are represented with second-order accuracy, while the inner walls are treated using a free-slip scheme in order to reduce the viscous boundary layer effects that result in a transfer of momentum by the tangential motion of particles along the walls. To ensure the numerical stability and to make the viscosity as small as possible, the relaxation time is set to $\tau = 0.5714$, which is equivalent to a dimensionless kinematic viscosity of $\nu = 0.0238$.² The undisturbed fluid density was set as $\rho_0 = 1.0 \text{ kg/m}^3$ for convenience.

The system is excited by a source signal that consists of a linear chirp signal running from $ka = 0.1$ to $ka = 3.8$ (up

² The physical kinematic viscosity is related to the dimensionless kinematic viscosity by $\nu^* = \frac{\nu c_s^* D_x}{c_s}$, where c_s^* is the physical speed of the sound, c_s is the speed of sound in lattice unit, D_x is the ratio of the physical length and the lattice length.

to the cut-on frequency of the first symmetric non-planar axial mode) superimposed on a DC offset representing the non-zero mean flow. The excitation is implemented by a source buffer at the left end of the pipe using absorbing boundary conditions with a non-zero target velocity prescribed by the source signal. Before the acoustic source is superimposed, there should be enough initialization time to allow the fluid in the whole domain to accelerate from stagnation to a stationary state. The minimum initialization steps can be estimated by

$$N_t \sim N_{t0} + L_x / (M * c_s),$$

where $N_{t0} = 4000$ is the acceleration time for the source buffer with thickness equivalent to 60 cells [14], $c_s = 1/\sqrt{3}$ is the speed of sound in lattice units, M is the Mach number of the non-zero mean flow and $L_x = 1000$ is the maximum traveling distance of the plane sound wave in the radiation domain in this system. For example, the minimum initialization steps corresponding to the Mach number of $M = 0.036$ is $N_t = 5.21 \times 10^4$. The highest Mach number used in this paper is $M = 0.15$, which makes the flow slightly compressible. However, the numerical model is still valid because the slightly unsteady compressible form of the Navier-Stokes equations can be fully recovered from the isothermal form of the Boltzmann equation by performing the Chapman-Enskog expansion, as described in [21] and [20].

The time histories of fluid density are probed at 75 points evenly distributed around the semi-circle (corresponding to angle increments of 2 degrees), with the center point at the outlet of the duct in the range of $\theta = 0^\circ$ to $\theta = 150^\circ$. The measuring distance is $d = 250$ cells from the outlet. The acoustic pressure p is calculated by

$$p(\theta, t) = (\rho(\theta, t) - \rho_0)c_s^2, \quad (1)$$

where $\rho(\theta, t)$ is the spontaneous fluid density and ρ_0 is the equilibrium density. For the case of zero mean flow, ρ_0 is nearly a constant and usually has the value of 1. For non-zero mean flow, however, ρ_0 in the vicinity of the probing points fluctuates over time and the fluctuating density can not be calculated by simply subtracting 1 from the spontaneous fluid density. For such a case, a zero-phase DC-blocking filter can be used to remove the offset caused by the flow.

Once the time history of acoustic pressures has been obtained, the pressure directivity can be calculated by

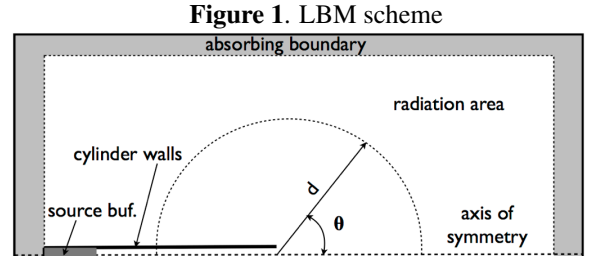
$$G(\theta, f) = \frac{P(\theta, f)}{P_h}, \quad (2)$$

where $P(\theta, f)$ is obtained by performing a DFT on the time history of sound pressure $p(\theta, t)$ measured at the same distance d , $P_h = \sqrt{\sum P^2(\theta)/N}$ is the square root of the averaged value of $P^2(\theta, f)$ over all the measured angles.

3. RESULTS

3.1 Directivity in the absence of mean flow

The LBM scheme in the absence of mean flow is first validated by comparing its results with the established analytical model proposed by Levine and Schwinger [1] in



the form of relative pressure directivity. For six different frequencies expressed in terms of the Helmholtz number ($ka = 0.48, 1, 2, 2.5, 3, 3.5$) that are below the cut-on frequencies of higher-order modes, the numerical simulations are in good agreement with the analytical results, as shown in Fig. 2. The tiny ripples found for $ka = 0.48$ and $ka = 1$ in the numerical results can be explained by the fact that $G(\theta)$ should be measured in the far-field condition, which is not fully satisfied for low frequencies given the size of the lattice (1000×500 cells) and the measuring radius (250 cells) used in this paper (due to computation time limits). Not surprisingly, the results for higher frequencies ($ka \geq 2$) are smooth and the ripples are barely observed. To evaluate the far-field condition in this simulation, we measured the acoustic impedance Z as a function of ka at a distance $d = 250$ and angle $\phi = 0$ from the outlet of the pipe. As depicted in Fig. 3(a), the amplitude of the impedance Z quickly converges to the characteristic impedance of the medium, $Z_c = \rho_0 c_s^2$, for values of $ka \geq 1$. A similar phenomenon can be found for the phase between the acoustic pressure and particle velocity, ϕ , which gradually converges to zero for $ka \geq 2$, as depicted in Fig. 3(b). The results suggest that the far-field condition is not fully satisfied for $ka < 1$, while for $ka \geq 1$, the acoustic impedance Z of the spherical wave propagating into the radiation domain approximates that of a plane wave.

From Fig. 2(f), we can observe smoothing of directivity characteristics of numerical results in the vicinity of $\theta = 100^\circ$ compared to that of the analytical results for the high frequency $ka = 3.5$. That might be attributed to the issue that, in the numerical simulation, there may be some transfer of energy from the exciting chirp signal to higher-order modes, while for the case of the analytical model, no higher modes are involved and the energies are exclusively coming from the dominant plane mode. A similar phenomenon was reported in a recent experimental measurement conducted by Gorazd et al. [3], where the curves presenting the directivity characteristics of the experimental results (excited by broadband noise) around $\theta = 100^\circ$ and for higher frequencies ($ka \geq 2.96$) are smoothed comparing to those analytical results obtained for a single-frequency exciting signal.

In the next step, the numerical and analytical results are compared with the experimental results by Gorazd et al. [3] in the form of relative pressure directivity. The experiment involved an unflanged radiating waveguide set-up with free field conditions in an anechoic chamber, which is comparable to the solid pipe wall and absorbing boundary con-

dition used in the numerical simulation. All three results (numerical, analytical and experimental) have been normalized to the same dB level, as depicted in Fig. 4. For the two lower frequencies of $ka = 0.74$ and 1.48 and for angles within the range of $0^\circ < \theta < 90^\circ$, the three results are in good agreement with each other, despite the fact that the measurements are carried out using 1/3 octave broadband noise and the calculation of numerical and analytical results are based on a single frequency. As the angle increases, the measurements are still in good agreement with the analytical results, though the numerical results have discrepancies less than 3 dB compared to the analytical results. For the higher frequency of $ka = 2.96$, the numerical results are in good agreement with both the analytical results and the measurements for angles within the range of $0^\circ < \theta < 75^\circ$. As the angle increases from 75° to 150° , both the measurements and the numerical results deviate from the analytical results, but in opposite ways. Compared to the analytical results, the highest discrepancies are found at the largest angle of $\theta = 150^\circ$, which is $+3.8$ dB for the measurements and -2.6 dB for the numerical results, respectively.

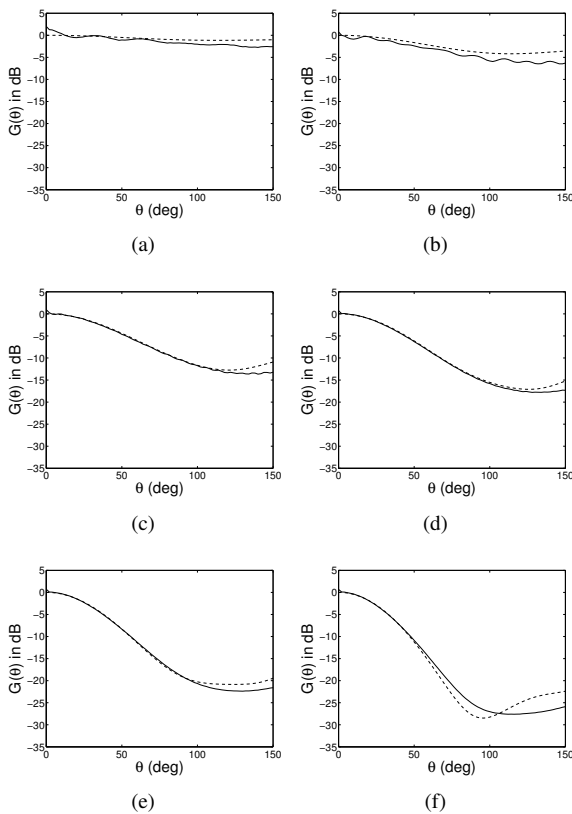


Figure 2. Comparison between numerical (solid) and analytical predictions [1] (---) of the acoustic pressure directivity as a function of the angle in the absence of a mean flow: (a) $ka = 0.48$, (b) $ka = 1$, (c) $ka = 2$, (d) $ka = 2.5$, (e) $ka = 3$, (f) $ka = 3.5$.

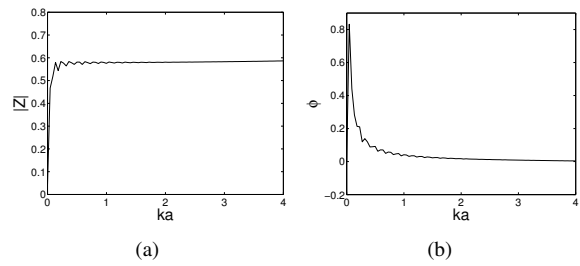


Figure 3. Evaluation of the far-field condition in terms of acoustic impedance in the radiation domain: (a) amplitude of acoustic impedance, (b) phase of acoustic impedance.

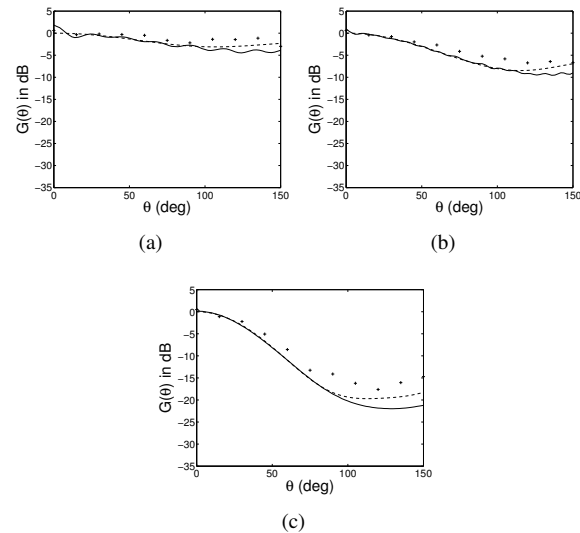


Figure 4. Comparison between numerical (solid), analytical predictions [1] (---) and experimental measurements [3] (+ + +) of the acoustic pressure directivity as a function of the angle in the absence of a mean flow: (a) $ka = 0.74$, (b) $ka = 1.48$, (c) $ka = 2.96$.

3.2 Directivity in the presence of mean flow

For the case of a cold mean flow with a low Mach number ($M = 0.036$), the numerical results are compared with the theoretical prediction given by Gabard and Astley [2] as well as the recent experimental results obtained by Gorazd et al. [3] in the form of normalized pressure directivity, as depicted in Fig. 5. All three results (numerical, analytical and experimental) have been represented in the form of pressure directivity and normalized to the same dB level.

In general, the results are in good agreement for angles in the range $0^\circ < \theta < 60^\circ$. Discrepancies between the numerical and analytical results become more obvious as the angle increases and the maximum differences are found to be at $\theta = 150^\circ$, i.e., -3.11 dB for $ka = 0.74$, -2.22 dB for $ka = 1.48$ and -2.3 dB for $ka = 2.96$, respectively. For all three frequencies and for most angles, the analytical solution is located between the numerical and the experimental results.

For the case of a cold mean flow with a higher Mach number ($M = 0.15$), the numerical results are compared with the theoretical prediction only, since no experimental re-

sults are available from Gorazd et al. for $M = 0.15$. The comparisons are depicted in Fig. 6. In general, good agreement is found for angles in the range $30^\circ < \theta < 150^\circ$. For most angles, the discrepancy from the theory is less than 3dB. The deviation of the simulation from the theoretical results is mainly found in the region of angles less than 30° . The smoothing of the curve representing the numerical results versus the analytical results in the region $90^\circ < \theta < 120^\circ$ for the high frequency of $ka = 3.77$, as depicted in Fig. 6(d), might be due to the transfer of energy from the exciting chirp signal to higher-order modes, as discussed before.

An important feature of the directivity characteristics in the presence of a non-zero mean flow concerns the so-called “zone of relative silence”, where the sound wave in the vicinity of the axis is subject to additional attenuation. The result from the theoretical analysis of Savkar [6] and Munt [4] suggests that, for high frequencies and large Mach numbers, the zone of relative silence is so obvious that a cusp can be observed at $\theta = \theta_s$ in the directivity pattern. Assuming that the medium outside the duct is stagnant and the speed of sound remains constant, the zone of relative silence is defined by [6]

$$\theta_s = \cos^{-1} \left(\frac{1}{1 + M} \right), \quad (3)$$

where M is the Mach number inside the duct.

Even for the low Mach number $M = 0.036$, the zone of relative silence ($\theta_s = 15.15^\circ$) can be observed in both the experiments and the numerical results for $ka = 2.96$, as depicted in Fig. 5(c). For the case of higher Mach number $M = 0.15$, the zone of relative silence ($\theta_s = 29.59^\circ$) is more obviously observed in the numerical results for all four frequencies ($ka = 0.74, 1.48, 2.96$ and 3.77).

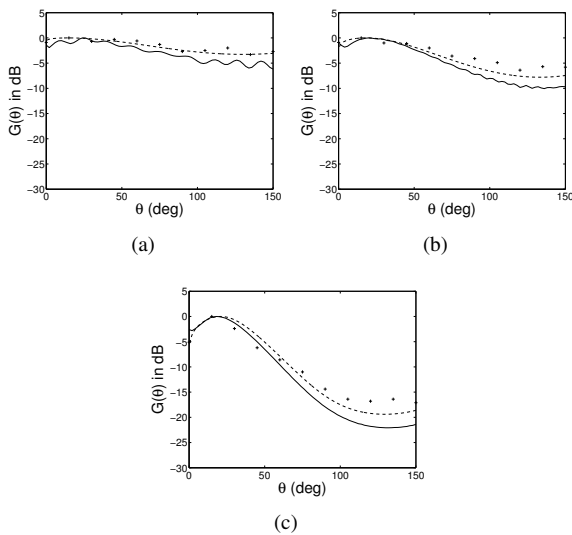


Figure 5. Comparison between numerical (solid), analytical [2] (---) predictions and experimental measurements [3] (+ + +) of the acoustic pressure directivity as a function of the angle in the presence of a mean flow at Mach = 0.036: (a) $ka = 0.74$, (b) $ka = 1.48$, (c) $ka = 2.96$.

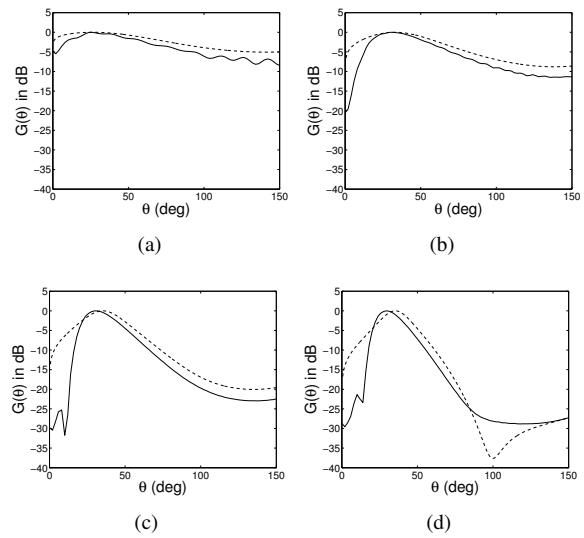


Figure 6. Comparison between numerical (solid) and analytical predictions [2] (---) of the acoustic pressure directivity as a function of the angle in the presence of a mean flow at Mach = 0.15: (a) $ka = 0.74$, (b) $ka = 1.48$, (c) $ka = 2.96$, (d) $ka = 3.77$.

4. CONCLUSIONS

In this paper, we presented a numerical technique based on an axisymmetric two-dimensional lattice Boltzmann scheme to predict the directivity pattern associated with the sound radiation at the open end of cylindrical ducts issuing a low Mach number cold subsonic jet into a stagnant fluid region.

The LBM scheme was first validated by comparing its results with the analytical model of Levine and Schwinger and experimental results of Gorazd et al. for the case of no flow. Then for the case of non-zero mean flow, the numerical results were compared with the theoretical prediction given by Gabard and Astley for Mach number $M = 0.036$ and $M = 0.15$ as well as experimental results obtained by Gorazd et al. for Mach number $M = 0.036$. Very good agreement was found with theoretical and experimental results for the case of no flow and the lower Mach number of $M = 0.036$. For the relatively higher Mach number of $M = 0.15$, the numerical result agrees very well with the theoretical prediction for angles greater than 30° , though significant discrepancies are observed for angles less than 30° . The effects of the so-called zone of relative silence are clearly observed in the results of non-zero mean flow even for very low Mach number ($M=0.036$). This is interesting for the studies of the sound radiation of woodwind instruments, which normally exhibit a very low Mach number flow.

The aforementioned discrepancies for the case of $\theta < 30^\circ$ and $M = 0.15$ are not well explained yet. For further investigations conducted by either experimental measurements or numerical simulations, some facts might be considered. The theoretical model assumes an infinitely thin vortex sheet separating the jet and the neighboring quiescent fluid, which is not true for far field in real situations as well as the numerical simulations presented here. In ad-

dition, it was found in the numerical simulation presented here that the directivity pattern in directions close to the axis is very sensitive to the probing distance.

Acknowledgments

The authors would like to thank Dr. Gwenael Gabard at University of Southampton, UK, for providing the numerical calculations of the theoretical model, and Mr. Lukasz Gorazd and Dr. Anna Snakowska at AGH University of Science and Technology, Poland, for providing the experimental data. We also wish to acknowledge funding from the Fonds québécois de la recherche sur la nature et les technologies (FQRNT), the Natural Sciences and Engineering Research Council of Canada (NSERC), and the Centre for Interdisciplinary Research in Music Media and Technology.

5. REFERENCES

- [1] H. Levine and J. Schwinger, "On the radiation of sound from an unflanged circular pipe," *Physical Review*, vol. 73, no. 4, pp. 383–406, 1948.
- [2] G. Gabard and R. J. Astley, "Theoretical model for sound radiation from annular jet pipes: far- and near-field solutions," *J. Fluid Mech.*, vol. 549, pp. 315–341, 2006.
- [3] L. Gorazd, J. Jurkiewicz, and A. Snakowska, "Experimental verification of the theoretical model of sound radiation from an unflanged duct with low mean flow," *Archives of Acoustics*, vol. 37, no. 2, pp. 227–236, 2012.
- [4] R. M. Munt, "The interaction of sound with a subsonic jet issuing from a semi-infinite cylindrical pipe," *J. Fluid Mech.*, vol. 83, no. 4, pp. 609–640, 1977.
- [5] S. Rienstra, "Acoustic radiation from a semi-infinite annular duct in a uniform subsonic mean flow," *J. of Sound and Vibration*, vol. 94, pp. 267–288, 1984.
- [6] S. D. Savkar, "Radiation of cylindrical duct acoustic modes with flow mismatch," *J. of Sound and Vibration*, vol. 42, no. 3, pp. 363–386, 1975.
- [7] M. Hornikx, W. De Roeck, and W. Desmet, "Simplified exhaust pipe noise radiation modelling using the fourier pstd method," in *International Conference on Noise and Vibration Engineering. Leuven, Belgium*, 2010, pp. 20–22.
- [8] X. Chen, X. Zhang, C. Morfey, and P. Nelson, "A numerical method for computation of sound radiation from an unflanged duct," *J. of Sound and Vibration*, vol. 270, pp. 573–586, 2004.
- [9] C. Rumsey, R. Biedron, and F. Farassat, "Ducted-fan engine acoustic predictions using a navierstokes code," *J. of Sound and Vibration*, vol. 213, no. 4, pp. 643–664, 1998.
- [10] Y. Ozyoruk and L. Long, "Computation of sound radiating from engine inlet," *American Institute of Aeronautics and Astronautics Journal*, vol. 34, no. 5, pp. 894–901, 1996.
- [11] P. A. Skordos, "Modeling flue pipes: subsonic flow, lattice boltzmann, and parallel distributed computers," Ph.D. dissertation, Massachusetts Institute of Technology, 1995.
- [12] A. R. da Silva and G. P. Scavone, "Lattice Boltzmann simulations of the acoustic radiation from waveguides," *J. Phys. A: Math. Theor.*, vol. 40, pp. 397–408, 2007.
- [13] A. R. da Silva, "Numerical studies of aeroacoustic aspects of wind instruments," Ph.D. dissertation, McGill University, Montreal, Canada, 2008.
- [14] A. R. da Silva, G. P. Scavone, and A. Lefebvre, "Sound reflection at the open end of axisymmetric ducts issuing a subsonic mean flow: A numerical study," *J. of Sound and Vibration*, vol. 327, pp. 507–528, 2009.
- [15] A. R. da Silva, G. P. Scavone, and A. Lenzi, "Numerical investigation of the mean flow effect on the acoustic reflection at the open end of clarinet-like instruments," *ACTA Acustica United with Acustica*, vol. 96, pp. 959–966, 2010.
- [16] R. M. Munt, "Acoustic transmission properties of a jet pipe with subsonic jet flow: I. the cold jet reflection coefficient," *J. of Sound and Vibration*, vol. 142, no. 3, pp. 413–436, 1990.
- [17] S. Allam and M. Abom, "Investigation of damping and radiation using full plane wave decomposition in ducts," *J. of Sound and Vibration*, vol. 292, no. 3-5, p. 519534, 2002.
- [18] M. C. A. M. Peters, A. Hirschberg, A. J. Reijnen, and A. P. J. Wijnands, "Damping and reflection coefficient measurements for an open pipe at low mach and low helmholtz numbers," *J. Fluid Mech.*, vol. 256, p. 499534, 1993.
- [19] S. Succi, *The lattice Boltzmann equation for fluid dynamics and beyond*. Oxford University Press, 2001.
- [20] D. A. Wolf-Gladrow, *Lattice Gas Cellular Automata and Lattice Boltzmann Models: An Introduction. Lecture Notes in Mathematics*. Springer, Berlin / Heidelberg, 2004.
- [21] Y. Qian, D. d'Humieres, and P. Lallemand, "Lattice bkg models for navier-stokes equation," *Europhysics Letters*, vol. 17, no. 6, pp. 479–484, 1992.
- [22] E. W. S. Kam, R. M. C. So, and R. C. K. Leung, "Non-reflecting boundary conditions for one-step lbm simulation of aeroacoustics," in *27th AIAA Aeroacoustics Conference, 8-10 May 2006, Cambridge, Massachusetts*, 2006.

- [23] I. Halliday, L. A. Hammond, C. M. Care, K. Good, and A. Stevens, "Lattice boltzmann equation hydrodynamics," *Physical Review E.*, vol. 64, no. 011208, pp. 1–8, 2001.
- [24] T. Lee, H. Huang, and C. Shu, "An axisymmetric incompressible lattice bgk model for simulation of the pulsatile flow in a circular pipe," *International Journal for Numerical Methods in Fluids*, vol. 49, no. 1, pp. 99–116, 2005.
- [25] M. Bouzidi, M. Firdaouss, and P. Lallemand, "Momentum transfer of a Boltzmann-lattice fluid with boundaries," *Physics of Fluids*, vol. 13, no. 11, p. 3452, 2001.
- [26] P. Lallemand and L. S. Luo, "Lattice Boltzmann method for moving boundaries," *J. of Computational Physics*, vol. 184, pp. 406–421, 2003.